geoconvention
Calgary • Canada • June 20-22 2022

Hybrid Foreshock Patterns of Injection-Induced Earthquakes in Western Canada

Bei wang[1,2], Honn Kao[1,2], Hongyu Yu[1], Ryan Visser[3]
[1]Geological Survey of Canada, Natural Resources Canada
[2]School of Earth and Ocean Sciences, University of Victoria, BC, Canada
[3]Geoscience BC, Canada

Summary

Foreshocks, which usually precede the mainshock by a short period of time ranging from a few hours to several days [Abercrombie and Mori, 1996; Jones, 1984; Mori and Abercrombie, 1997], are probably the most important precursory phenomena hinting the imminent major ruptures. Thus, understanding the source characteristics and seismogenic pattern of foreshock sequences is crucial to the success of short-term earthquake forecast and hazard mitigation.

Since early 2000s, injection-induced earthquakes (IIE) associated with the development of unconventional hydrocarbon resources have drawn serious public and regulatory concerns due to their increasing trend in both magnitude and occurrence frequency. Despite that the seismogenic process of IIE has been a research focus for years [e.g., Eyre et al., 2019; Schultz and Eaton, 2018; Segall and Lu, 2015], there has been a lack of systematic investigation into the occurrence and seismogenic patterns of their foreshocks. In the Western Canadian Sedimentary Basin, a coordinated effort has been made to strengthen monitoring of the drastic increase of hydraulic fracturing (HF)-related IIE in the region [e.g., Farahbod et al., 2014]. Moreover, new earthquake detection and location techniques have been deployed to create a much-enhanced earthquake catalog for northeast British Columbia (NEBC), lowering the earthquake detection threshold by at least one magnitude unit [Mahani et al., 2016]. The remarkable improvement in both quality and quantity of the regional seismic data allows us to identify and locate precursory seismicity of IIE at unprecedent resolution

In this study, we examine the occurrence pattern of foreshocks for relatively large (M ≥3) IIE in NEBC. We first apply the Source-Scanning Based on Navigated Automatic Phase-Picking method [*Tan et al.*, 2019] on continuous waveforms from local seismic stations to locate earthquakes in the study area from 2014 to 2021. Our catalogue has more than 20,000 events in total, with 19 of them being M≥3 (Fig.1a). Then, we set a spatiotemporal criterion of 3 km and 5 days to associate foreshocks with each M≥3 mainshock. To further improve the foreshock detection, we also deploy a template matching method to identify uncatalogued events within the 5-day time window preceding each mainshock.

Overall, our results suggest that foreshock activities are pervasive in NEBC. The vast majority of major IIE sequences (16 out of 19, ~84%) contain foreshocks (Fig. 1). Particularly, we find 80% of the mainshocks in the northern Montney play are accompanied with foreshocks (13/16),

whereas all mainshocks in the southern Montney play have foreshocks (3/3). Another interesting observation is that the number of foreshocks varies significantly for the 16 mainshocks. For example, the M3.2 mainshock on 11 September 2020 has more than 700 foreshocks. There are another 5 mainshocks with more than ~180 foreshocks. In contrast, the remaining 9 mainshocks have about an order less foreshocks, ranging from 3 to 23.

Next, we try to identify the physical factors that correlate with the variation of observed IIE foreshock patterns. The most obvious controlling factor is the timing of fluid injection. Foreshocks tend to occur during or immediately after individual injections (Fig. 2a). We also observe more foreshock activities in areas with higher seismogenic index (Fig. 2b). Finally, we calculate the β-value for each 1º-by-1º cell to identify areas where dynamic triggering of local earthquakes occurs, following the method in Wang et al. (2018). Generally speaking, a β-value of >2 suggests that the phenomenon of dynamic triggering is statistically significant. Our results indicate that the level of foreshock activity appears to be higher in areas where dynamic earthquake triggering is also observed (Fig. 2c).

There are two major theories in seismology to explain the underlying physical mechanism relating foreshocks to the development of mainshock: the cascade model and the pre-slip model [*Chen and Shearer*, 2016; *Ellsworth and Bulut*, 2018; *Seif et al.*, 2018]. In the cascade model, each foreshock is responsible for triggering the next foreshock in the neighborhood through static stress transfer that eventually leads to the mainshock [e.g., *Ellsworth and Bulut*, 2018]. In the pre-slip model, however, foreshocks and the corresponding mainshock are both caused by quasi-steady slip within an extended area without a clear sequential relationship in space [e.g., *Dodge et al.*, 1996; *Tape et al.*, 2018]. Our results indicate that some foreshock-mainshock sequences can be explained by the cascade model while others are more consistent with the pre-slip model. This hybrid pattern probably implies that the seismogenic development of IIE sequences can be accomplished by different physical mechanisms depending on the local geological, hydrological, and geomechanical conditions.

Our results have important strategy implications for effective mitigation of seismic hazard due to IIE. In areas where foreshocks are commonly observed before mainshocks, enhanced seismic monitoring during and after injection operations should be required to capture the precursory signals before runaway ruptures are initiated. In areas where IIE mainshocks occur without foreshocks, the regulatory Traffic Light Protocol probably should consider including additional parameters to become more effective.

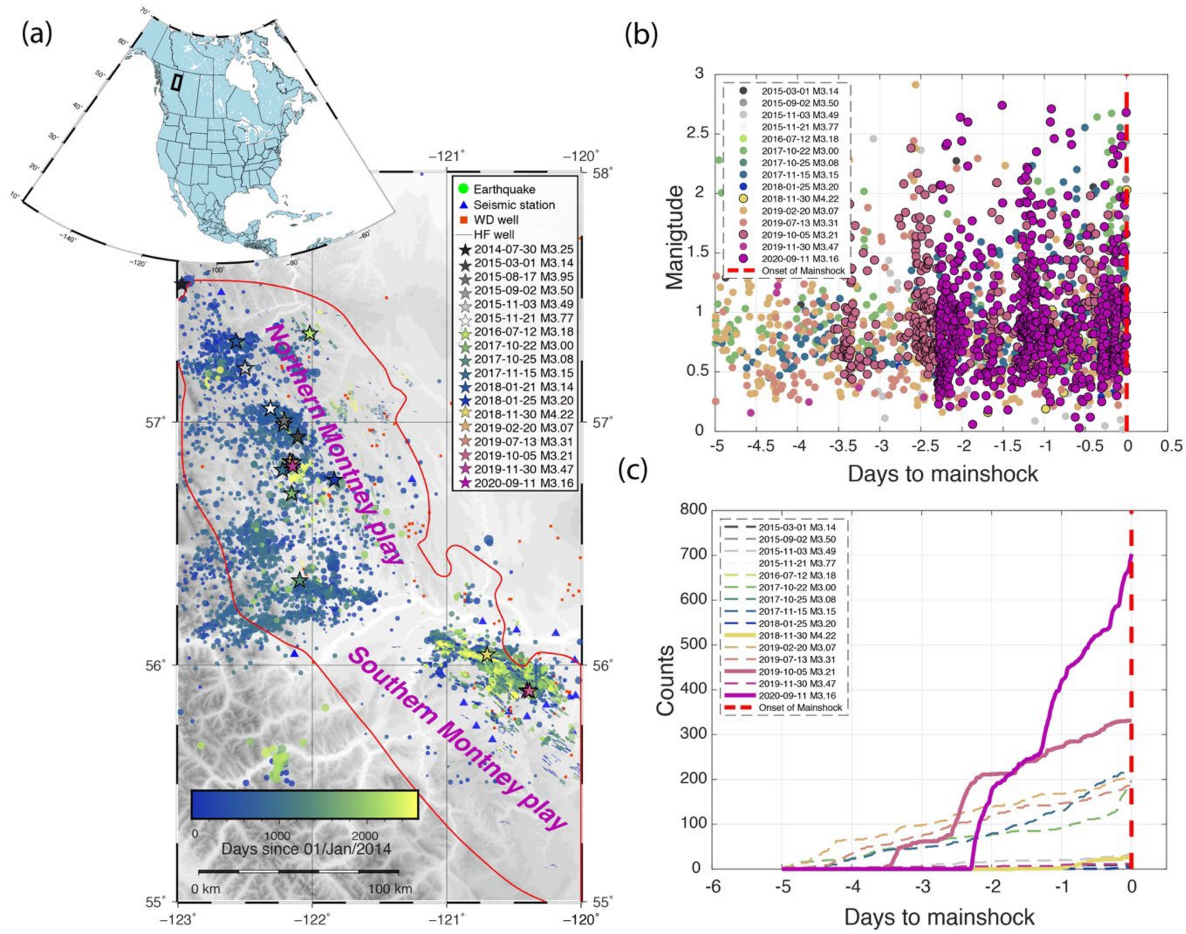

Figure 1. (a) Seismicity and seismic stations in northeastern British Columbia for the period 2014-2020. Circles denote earthquake epicenters. Blue triangles show the location of seismic stations. Short lines and red squares show the location of HF wells and WD pads, respectively. Earthquake symbol size corresponds to its magnitude. Earthquakes and HF wells are colored with respect to 01 Jan 2014. Red line marks the boundary of the Montney play. The colored stars correspond to M≥3 mainshocks in our study area. (b) Scatter plot of events detected by the S-SNAP method and template matching method. Different colors mean different foreshock-mainshock sequences. The X-axis corresponds to the time before the respective mainshock, which is marked by a red dashed line at t=0. (c) The cumulative number of foreshocks for different IIE sequences. Color scheme is the same as that in (a).

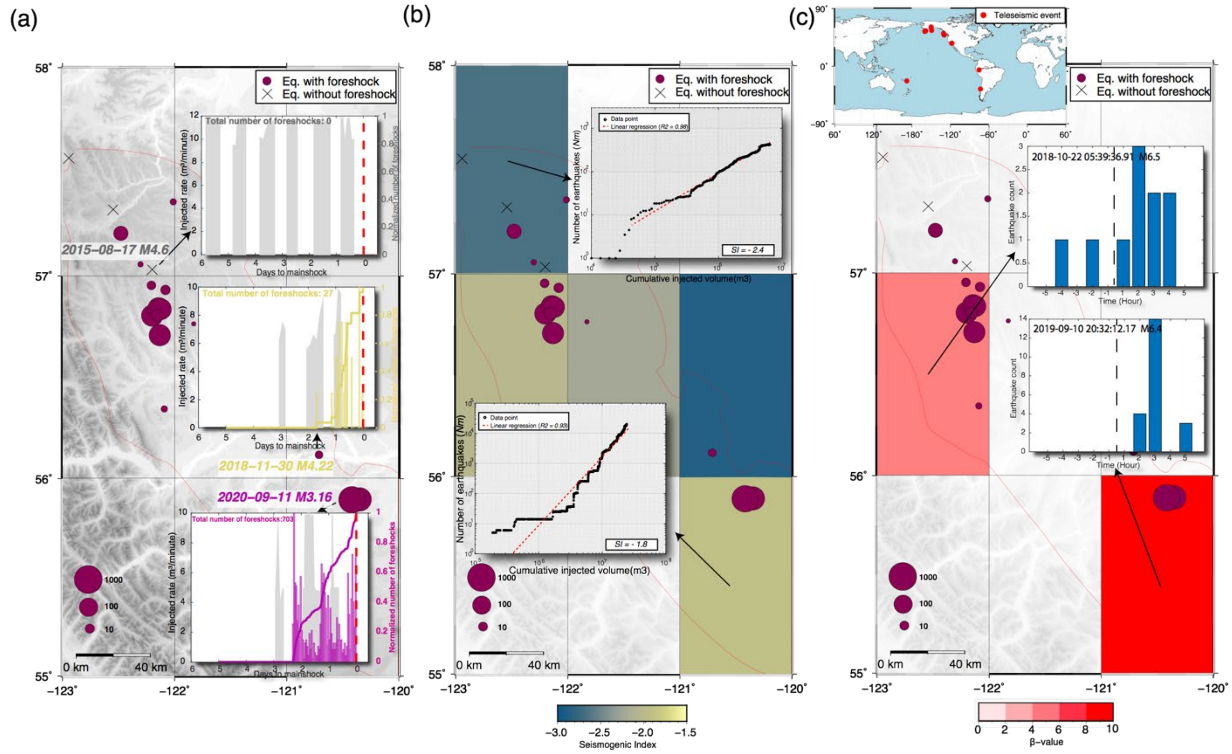

Figure 2. Maps showing the epicenters of M≥3 IIE (circles) in the Montney Play. (a) Topography as the background with three insets from top to bottom showing three different foreshock scenarios: no, few and many foreshocks before the mainshock. (b) Seismogenic index as the background. Two insets show the relationship between the accumulated number of events and injected volume for two representative areas where the seismogenic index is low and high, respectively. (c) β-value as the background. Two insets show the detailed temporal distribution of local earthquakes before and after two major teleseismic earthquakes. Dashed lines mark the origin times of the teleseismic events.

References

Abercrombie, R. E., and J. Mori (1996), Occurrence patterns of foreshocks to large earthquakes in the western United States, *Nature*, *381*(6580), 303-307, doi:10.1038/381303a0.

Chen, X., and P. M. Shearer (2016), Analysis of Foreshock Sequences in California and Implications for Earthquake Triggering, *Pure and Applied Geophysics*, *173*(1), 133-152, doi:10.1007/s00024-015-1103-0.

Dodge, D. A., G. C. Beroza, and W. L. Ellsworth (1996), Detailed observations of California foreshock sequences: Implications for the earthquake initiation process, *Journal of Geophysical Research: Solid Earth*, *101*(B10), 22371-22392, doi:10.1029/96JB02269.

Ellsworth, W. L., and F. Bulut (2018), Nucleation of the 1999 Izmit earthquake by a triggered cascade of foreshocks, *Nat. Geosci.*, *11*(7), 531-535, doi:10.1038/s41561-018-0145-1.

Eyre, T. S., D. W. Eaton, D. I. Garagash, M. Zecevic, M. Venieri, R. Weir, and D. C. Lawton (2019), The role of aseismic slip in hydraulic fracturing-induced seismicity, *Sci Adv*, *5*(8), eaav7172, doi:10.1126/sciadv.aav7172.

Farahbod, A. M., J. F. Cassidy, H. Kao, and D. Walker (2014), Collaborative studies of regional seismicity in northeast British Columbia, *Can. Soc. Explo. Gephys. Recorder*, *39*, 40-44.

Jones, L. M. (1984), Foreshocks (1966-1980) in the San Andreas system, California, *Bulletin of the Seismological Society of America*, *74*(4), 1361-1380, doi:10.1785/bssa0740041361.

Mahani, A. B., H. Kao, D. Walker, J. Johnson, and C. Salas (2016), Performance Evaluation of the Regional Seismograph Network in Northeast British Columbia, Canada, for Monitoring of Induced Seismicity, *Seismological Research Letters*, *87*(3), 648-660, doi:10.1785/0220150241.

Mori, J., and R. E. Abercrombie (1997), Depth dependence of earthquake frequency-magnitude distributions in California: Implications for rupture initiation, *Journal of Geophysical Research: Solid Earth*, *102*(B7), 15081-15090, doi:10.1029/97JB01356.

Schultz, R., and D. W. Eaton (2018), Increased likelihood of induced seismicity in highly overpressured shale formations, *Geophysical Journal International*, *214*(1), 751-757, doi:10.1093/gji/ggy167.

Segall, P., and S. Lu (2015), Injection-induced seismicity: Poroelastic and earthquake nucleation effects, *Journal of Geophysical Research: Solid Earth*, *120*(7), 5082-5103, doi:10.1002/2015JB012060.

Seif, S., J. D. Zechar, A. Mignan, S. Nandan, and S. Wiemer (2018), Foreshocks and Their Potential Deviation from General Seismicity, *Bulletin of the Seismological Society of America*, *109*(1), 1-18, doi:10.1785/0120170188.

Tan, F., H. Kao, E. Nissen, and D. Eaton (2019), Seismicity ‐ Scanning Based on Navigated Automatic Phase ‐ Picking, *Journal of Geophysical Research: Solid Earth*, *124*(4), 3802-3818, doi:10.1029/2018jb017050.

Tape, C., S. Holtkamp, V. Silwal, J. Hawthorne, Y. Kaneko, J. P. Ampuero, C. Ji, N. Ruppert, K. Smith, and M. E. West (2018), Earthquake nucleation and fault slip complexity in the lower crust of central Alaska, *Nature Geoscience*, *11*(7), 536-541, doi:10.1038/s41561-018-0144-2.

Wang, B., R.M. Harrington, Y. Liu, H. Kao, and H. Yu (2018). Remote Dynamic Triggering of Earthquakes in Three Unconventional Canadian Hydrocarbon Regions Based on a Multiple-Station Matched-Filter Approach. *Bulletin of the Seismological Society of America* 109, 372-386, doi:.